LEGIBILITY NOTICE

A major purpose of the Technical Information Center is to provide the broadest dissemination possible of information contained in DOE's Research and Development Reports to business, industry, the academic community, and federal, state and local governments.

Although a small portion of this report is not reproducible, it is being made available to expedite the availability of information on the research discussed herein.

1

CONF - 830719 - - 1

MASTER

LA-UR--83-1584

DE83 014972

AUTHOR(S)   S. C. Schmidt, M-6
            D. S. Moore, CHM-4
            J. W. Shaner, M-6

Los Alamos

Los Alamos National Laboratory
Los Alamos, New Mexico 87545

RAMAN SPECTROSCOPIES IN SHOCK-COMPRESSED MATERIALS*

S. C. Schmidt, D. S. Moore and J. W. Shaner

Los Alamos National Laboratory
Los Alamos, New Mexico

Spontaneous Raman spectroscopy, stimulated Raman scattering and coherent anti-Stokes Raman scattering have been used to measure temperatures and changes in molecular vibrational frequencies for detonating and shocked materials. Inverse Raman and Raman induced Kerr effect spectroscopies have been suggested as diagnostic probes for determining the phenomenology of shock-induced chemical reactions. The practicality, advantages, and disadvantages of using Raman scattering techniques as diagnostic probes of microscopic phenomenology through and immediately behind the shock front of shock-compressed molecular systems are discussed.

INTRODUCTION

Raman spectroscopy is a potentially valuable experimental technique for determining the structure and energy transfer mechanisms dominant through and immediately behind the shock front during the shock-compression of molecular systems. In particular, it could help elucidate the microscopic physical and chemical behavior that occurs in this region and the coupling of the microscopic processes to hydrodynamic and energy transport phenomena. Understanding this phenomenology will require answering at least four key questions: (1) what are the molecular, crystal and defect structures in this region; (2) what are the intra- and inter-molecular energy transfer mechanisms and, as a corollary, what chemical reactions or phase transitions occur through this region?; (3) what is the coupling between microscopic processes and macroscopic phenomena such as hydrodynamic flow and radiative transport?; and (4) how do the unique features of the shock process influence and govern the chemistry and material changes that occur during shock-compression?

The goal of this paper is to discuss the practicality, advantages and disadvantages of Raman scattering techniques as diagnostic probes of the microscopic phenomenology through and immediately behind the shock front of shock-compressed molecular systems, thus generating some of the answers to these questions. We will review the results achieved to date using Raman spectroscopies and in particular will emphasize our recent work using backward stimulated Raman scattering and reflected broadband coherent anti-Stokes Raman scattering to measure vibrational frequency shifts of shock-compressed benzene.

Prior to discussing Raman scattering techniques, several problems associated with conducting condensed phase shock wave experiments are reviewed. For many materials shock

waves are believed to be of the order of 1 nm or less in thickness.[1] The passage time through the front of a shock whose velocity is 5 km/sec is thus of the order of 200 psec or less. Hence, if we desire temporal and spatial resolutions through a shock-front (5 data points), the diagnostic technique selected must be capable of spatial and temporal resolutions of 0.2 μ and 40 psec, respectively. If psec chemical reactions are dominant as is suspected for organic materials, the temporal resolution must be better. Within bandwidth and diffraction limits, optical techniques offer some potential for achieving spatially resolved fast temporal measurements. However, with such methods there are several complications. Many materials are opaque or become opaque when shock-compressed. Consequently, the use of optical diagnostic techniques will probably be limited to a few select materials primarily for phenomenology studies. These studies, however, may have tremendous potential when used in conjunction with other techniques for determining phenomenology of shock-compressed materials.

Two other difficulties inherent in using optical techniques for shock-wave diagnostics are the problem of changes in material refractive index that accompanies the density or phase changes characteristic of shock waves and the possibility of induced photochemistry when using optical probes. Figure 1 shows the difficulty encountered when attempting to pass an optical beam through a shock-compressed system. The trailing shock wave near the sample boundaries tends to bend the optical beam away from the shock-front thus making prediction of the expected optical path difficult. Any shock-front curvature will compound this difficulty. If the shock velocity in the window is greater than in the sample, additional complications could arise from the effect of the more complex wave structure on the window transmission. Many molecules exhibit photochemical behavior when subjected to light, particularly that in the ultraviolet region of the spectrum. If these reactions are fast compared to the characteristic time
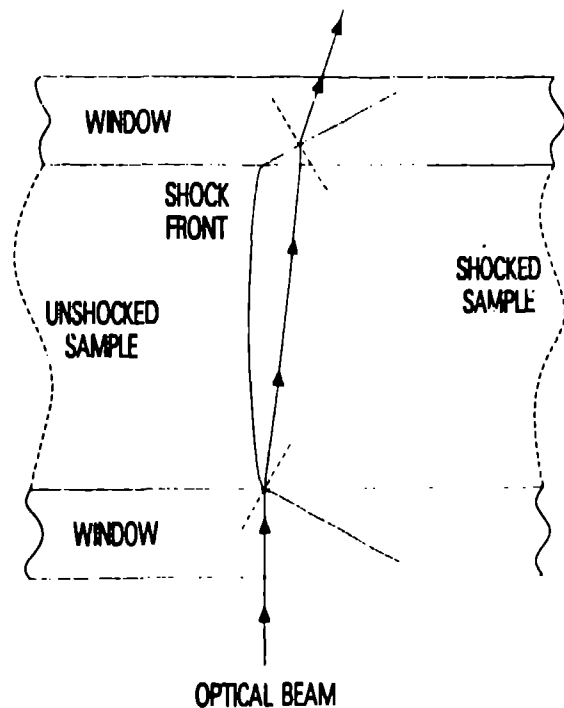
Figure 1. Refractive Effects Of Shock Wave On Optical Beam.

Labels in figure: WINDOW, SHOCK FRONT, SHOCKED SAMPLE, UNSHOCKED SAMPLE, WINDOW, OPTICAL BEAM

of the optical diagnostic, measurements could include the effects of both the shock stimulus and the photochemical reaction.

Measurements made using nonhomogeneous samples often are averaged over the nonuniformities and consequently do not reflect the details of the microstructure. For materials like granular explosives the nonhomogeneous nature is readily apparent and experiments are interpreted accordingly. For samples thought to be homogeneous, ambiguities can arise. For
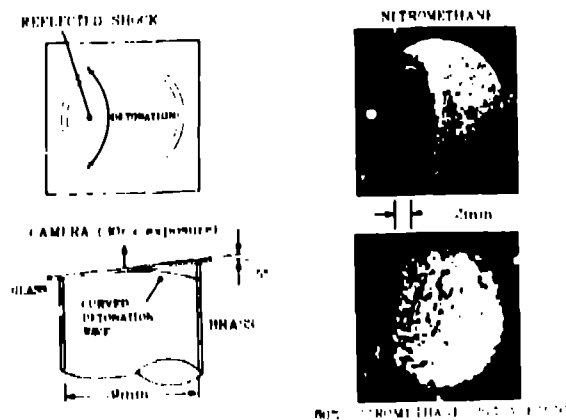

Figure 2. Detonation Wave Microstructure For Nitromethane And A Nitromethane/ Acetone Mixture [2]

example, Fig. 2 depicts two image-intensifier-camera pictures[2] of the shock-front of detonating nitromethane and an 80% nitromethane/ 20% acetone mixture. Liquids are often thought to be homogeneous materials, however, these pictures show that microstructure exists in the vicinity of the shock-front. Nothing is known about the microstructure in the region immediately behind the front. When performing experiments on nitromethane or similar substances, especially experiments utilizing optical techniques where spatial resolutions of tens of microns are desired, one must be aware that results may actually reflect an average over a smaller characteristic microstructure. Conversely, a single measurement with spatial resolution smaller than the microstructure may be misinterpreted as representative of the average material.

INCOHERENT RAMAN SCATTERING

Spontaneous Raman spectroscopy in shock-compressed systems was first performed in detonating crystalline Hexogene (RDX).[3] Subsequently the technique has been used to measure the temperature of detonating nitromethane[4] and to look at the frequency shift of vibrational bands of detonating pentrite (PETN) and RDX.[5,6] An attempt is presently under way to perform Raman scattering measurements in a medium which is shock-compressed using a high velocity gas gun.[7]

Raman scattering is the inelastic scattering of light from molecules. The scattering cross-section and hence the detection sensitivity are considerably smaller than for dipole emission/ absorption processes. The small scattering cross-section becomes particularly relevant when the scattering medium has a large background emission level such as might be true in a hot shock-compressed material. This difficulty can be overcome to some degree by using a short wavelength exciting frequency; however, care must be taken to avoid interfering fluorescence from photochemically produced species.

Since Raman scattering occurs into 4π steradians, detection can be made at an angle to the exciting beam so that spatial resolution is determined by either the diffraction limit of the optical components or the sensitivity of the detector and the magnitude of the scattering cross-section. This is a significant advantage compared to dipole emission/ absorption techniques where the observed effect results from emission/ absorption along a path length. Temporal resolution is limited by the sensitivity of the detector, the pulse duration of the exciting laser and the magnitude of the scattering cross-section. A resolution of approximately 10 nsec was achieved in detonating PETN.[5,6] Figure 3 shows schematically the Raman scattering experiments[5,6] used to measure temperatures via

STOKES, ANTI-STOKES RAMAN SPECTRUM
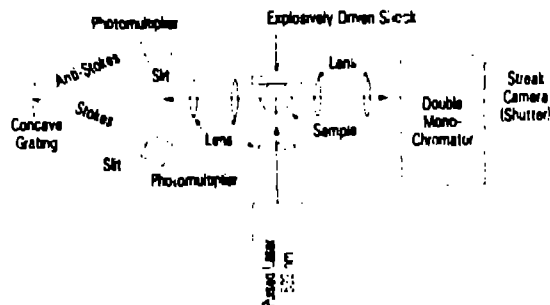INTENSITY RATIO

Figure 1. Spontaneous Raman Scattering Experiments.[4-6]

Stokes-anti-Stokes intensity ratios and vibrational frequency shifts for shock-compressed detonating materials. For both experiments scattering was observed at 90° to the incident exciting radiation. Temporal resolution was of the order of 10 nsec and a 30 nsec window was observed in which measurements could be made before the intense light emitted by the detonation front gave a large background intensity. Based on a PETN detonation velocity of 8 km/sec this implies the observation region was about 250 microns long. The detonator was the major source of timing uncertainty. Overlap of the laser pulse with the 30 nsec window could be improved by using a more precise triggering scheme for Q-switching the laser. The information which can be gained from these kinds of experiments is primarily the shifts in molecular energy levels resulting from shock-compression and an estimate of the vibrational temperature in the region behind the shock-front. Although good spatial resolution is possible, there are still difficulties because refractive index effects, as depicted in Fig. 1, make precise optical alignment difficult. Coupling these problems with a small scattering amplitude appears to limit the potential of ordinary Raman scattering for making precise spatial measurements, particularly measurements through the shock-front and the detection of species with small concentrations. Advantages and disadvantages of spontaneous Raman scattering are given in Table I.

Resonance Raman scattering occurs when the exciting frequency is in resonance or near resonance with an actual transition of the system.[8,9] For discrete and continuum resonance Raman scattering, the scattered intensity can increase dramatically, both for fundamentals and overtones. The emission intensity can also become large due to the onset

of resonance fluorescence. In addition, for discrete resonance Raman scattering, since laser radiation is being absorbed by the sample, complications from photochemistry and sample heating can be expected. Time resolved nsec and psec resonance Raman spectroscopy experiments[9,10] have been performed in dilute solutions at ambient conditions. Generally signal averaging was used to improve signal-to-noise ratios. Pulsed resonance Raman scattering measurements may be possible in shock-compressed systems to determine vibrational fundamentals and overtones of small concentration species. However, gating of the detector might be required to eliminate fluorescence effects. Also, results of single pulse experiments,[9] while improved compared to spontaneous Raman scattering intensities do not show signal-to-noise ratios as large as observed using the coherent techniques discussed later in this paper (Table I).

COHERENT RAMAN SPECTROSCOPY

Several coherent Raman scattering techniques have been demonstrated (Fig. 4). Advantages of these techniques, primarily due to large scattering intensities (Table I) and minimal experimental complications, are increased detection sensitivity, temporal resolution limits approaching laser pulse durations and possible spatial resolution approaching the diffraction limit of the optical components. As with all optical methods, optical accessibility (i.e., because of opacity) remains a major difficulty with the coherent Raman techniques.

Backward-stimulated Raman scattering (BSRS) has been observed in shock-compressed benzene.[11] Stimulated Raman scattering[12,13] (Fig. 4) occurs when the incident laser intensity in a medium exceeds a threshold level and generates a strong, stimulated, Stokes beam. The threshold level is determined by the Raman cross-section and linewidth of the transition and by the focusing parameters of the incident beam. Typical threshold intensities are ~ 10-100 GW/cm². Figure 5 illustrates the arrangement used for a backward stimulated Raman scattering experiment. An aluminum projectile of known velocity from a 51-mm-diam. light-gas gun impacted an aluminum target plate producing a shock wave which ran forward into a 9 to 11-mm-thick benzene sample. Standard data reduction techniques[14] using published shock-velocity/particle-velocity data were used to determine the state of the shock-compressed benzene. A single 6-ns-long frequency-doubled Nd-doped yttrium aluminum garnet (Nd:YAG) laser pulse was focused through the quartz window to a point in the benzene 2 to 6 mm in front of the rear sample wall. The timing sequence was determined by the incoming projectile. Interruption of a HeNe laser beam, in conjunction with an appropriate time delay, triggered the laser flash lamp approximately 100 μs prior to

impact. A time-of-arrival pin activated just before impact and the appropriate time delay served to Q switch the laser just prior to the shock wave striking the quartz window and after it was well past the focal point of the incident laser light.

In liquid benzene, the ν_1 symmetric stretching mode[16] at 992 cm^{-1} has the lowest threshold for stimulated Raman scattering induced by 532-nm light, and was the transition observed in these experiments. As depicted in Fig. 5, the backward stimulated Raman beam was separated from the incident laser by means of a dichroic filter and was then focused onto the 10-μ-wide entrance slit of a 1-m Czerny-Turner spectrograph equipped with a 1200-grooves/mm grating used in first order. Figure 6 shows the resulting spectrogram for benzene shock-compressed to 0.92 GPa. The reflected incident laser line and the backward stimulated Brillouin-scattering line at 532 nm are observable, as are the backward stimulated Raman-scattering line from the shocked sample and the backward stimulated
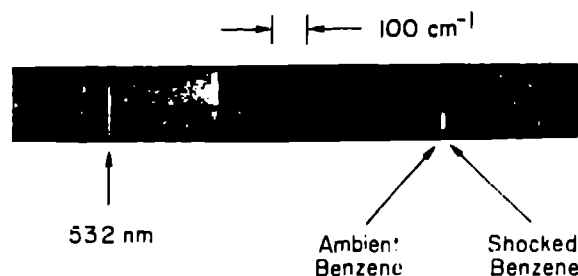
COHERENT RAMAN SCATTERING

Figure 4.   Coherent Raman Scattering Techniques.

Figure 5.   Backward Stimulated Raman Scattering Experiment.

Figure 6.   Scattered Light Spectrogram For Shock-Compressed Benzene.[11]

Raman-scattering line from ambient benzene. The latter feature resulted as a consequence of the shock wave having passed only about two-thirds of the way through the sample, and hence a stimulated Raman signal was also obtained from the unshocked liquid.

The frequency shift of the Raman line will have small contributions of approximately 0.1 cm^{-1} because the light crosses the moving interface between two media of different refractive indices and because the material behind the shock wave was moving.[17] Since these errors are considerably less than the experimental uncertainty of ± 0.5 cm^{-1} for the measured frequency shifts and are a small fraction of the shift due to compression, no attempt was made to correct the data for these effects.

Figure 7 gives the measured shift of the ν_1 ring-stretching mode vibrational wave number versus pressure of the shocked benzene. Observation of the ring-stretching mode at 1.18 GPa strongly suggests that benzene molecules still existed several millimeters behind the shock wave at this pressure, but does not, however, exclude some decomposition.[18]

Signal beam intensities using BSRS are sufficiently large that film can be used as a detector. The large incident intensities required, however, can cause damage to optical components near focal points. Spatial and temporal resolution (Table I) are determined by the confocal parameter of the focusing lens and the incident laser pulse duration. The BSRS technique also suffers from the difficulty that only certain molecules produce stimulated Raman scattering and of those molecules only the lowest threshold transition produces scattering. Therefore, stimulated Raman scattering is probably best used as a diagnostic to look at single select species in the steady region behind the front of a supported shock.

Inverse Raman or stimulated Raman loss spectroscopy[19,20] (Fig. 4) has been suggested[21] as a diagnostic technique for shock-compressed systems. Scattering can occur at

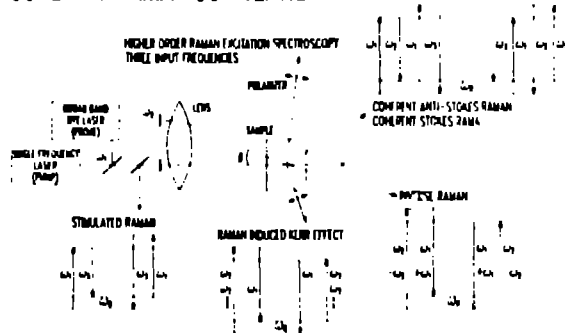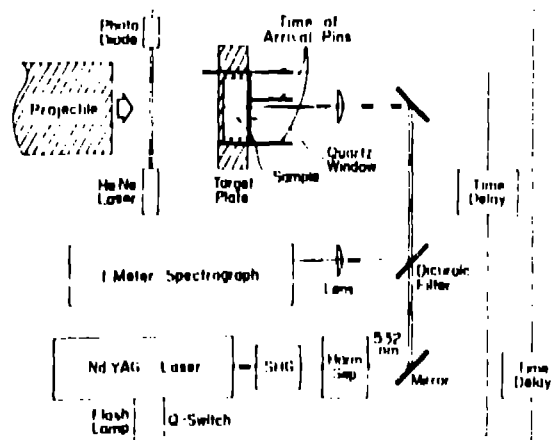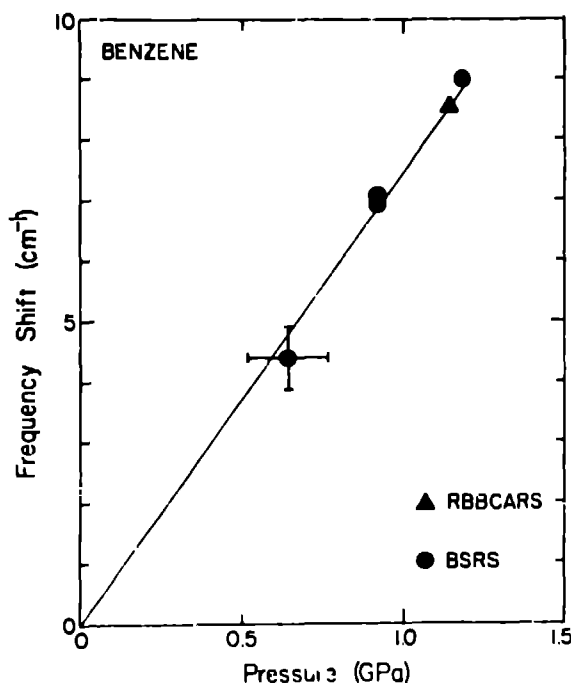Figure 7. Benzene Ring-Stretching Mode Vibrational Frequency Shifts (With Respect To 992 cm^{-1}) Versus Pressure.[1,24] Data Recorded Using BSRS And RBBCARS Are Denoted By Circles And Triangles, Respectively. The Single Triangle For RBBCARS Represents Two Data Points. Uncertainties In The Data Are Given On One Data Point.

incident power levels considerably below those required for stimulated Raman scattering by overlapping the pump beam with a beam, usually a broad band source, at the anti-Stokes frequency. Radiation is scattered from the broad band source (appears as an absorption) into the pump frequency. No threshold intensity exists as in the case of stimulated Raman scattering, hence, the complete Raman-active spectrum, with sufficient intensity to overcome fluorescence and other background effects, should thus be visible.

Since phase matching is not required as in many of the coherent techniques discussed later, several geometric arrangements are possible. Spatial and temporal resolution (Table I) should be the diffraction limit of the optical components and the laser pulse length, respectively. A difficulty does arise with the inverse Raman technique when a broadband dye laser is used for the Stokes beam. Roughness or irregularities of the intensity of the continuum, due to etalon behavior of the optics in the laser and thermal gradients in the dye stream, can be of the order of the absorption signal, thus adversely

affecting spectral resolution and detection sensitivity.

Coherent anti-Stokes Raman scattering (CARS) and coherent Stokes Raman scattering (CSRS)[22,23] (Fig. 4) occur as four-wave parametric processes in which three waves, two at a pump frequency and one at either the Stokes or anti-Stokes frequency are mixed in a sample to produce a coherent beam at the anti-Stokes or Stokes frequency, respectively. The mixing is greatly enhanced if the frequency difference between the pump and the Stokes or anti-Stokes frequencies coincides with a Raman active mode of the sample. Like inverse Raman scattering, CARS and CSRS can be produced at incident power levels considerably below those required for stimulated Raman scattering. however, since phase matching is required, possible geometrical arrangements are limited.

Figure 8 depicts an experiment used to measure CARS in shock-compressed liquid benzene and mixtures of benzene and benzene-d$_6$.[24] The gas gun described previously was used to accelerate a magnesium projectile with an 8-mm thick 304 stainless steel warhead to a desired velocity. The projectile struck a 2.1-mm thick 304 stainless steel target plate producing a shock wave which ran forward into a 7.5 to 8.0-mm thick benzene (or mixture) sample. Stainless steel was chosen because previous experience has shown it to retain its reflectivity under shock compression. The state of the shock-compressed samples was determined using published shock-velocity/particle-velocity data.[15] Mixture densities were determined according to volume fraction of benzene and benzene-d$_6$. The timing sequence for the RBBCARS experiment differed from that of BSRS experiments in that aluminum time-of-arrival pins replaced the HeNe laser beam triggering system. Since the Raman fre-
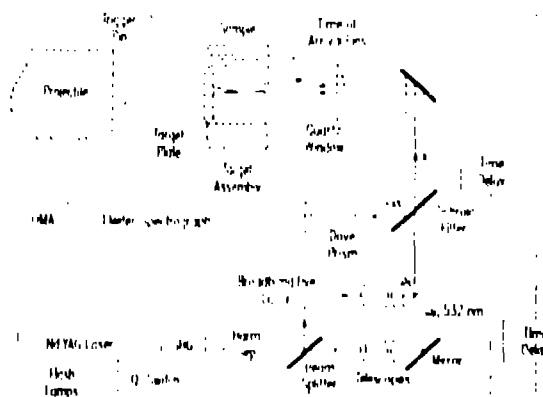

Figure 8. Reflected Broad-Band Coherent Anti-Stokes Raman Scattering Experiment.[24]

quencies of the shock-compressed materials are not precisely known, and since we wished to produce CARS signals from more than one mode or species, a broad-band dye laser, with a bandwidth equivalent to the gain profile of the dye, was used as the Stokes beam.[25] A portion of the 6 ns long frequency doubled Nd:YAG laser pulse was used to pump the dye laser. The resulting two laser beams (dye and remaining pump) were passed through separate Galilean telescopes and sent along parallel paths towards the sample. The beams were focused and crossed (with approximately 1 mm length of overlap) at a point 4 mm in front of the rear sample wall using a previously described technique.[26] The beam crossing angle (phase-matching angle) was tuned by adjusting the axial distance between the parallel beams using a precision translation stage on the dye laser beam turning prism. The CARS beam was reflected out of the shocked sample by the highly polished front surface of the target plate and along a path parallel to the two incoming beams. After being separated from the pump and Stokes beams using a long-wavelength-pass dichroic filter, the beam was then passed through a dove prism and focused onto the 75μm wide entrance slit of the spectrometer. The dove prism was used to rotate the image of the CARS signal so that any beam movement resulting from the changing position of the reflecting surface during the shock-compression process would translate to movement along, rather than across, the spectrometer entrance slit. The signals were detected at the exit of the spectrometer using a silicon-intensified-target vidicon (EGG-Par 1205D) coupled to an optical multi-channel analyzer (OMA) (EGG-PAR 1205A).

Figure 9 shows the OMA recorded RBBCARS signals for the ring-stretching modes of benzene and benzene-d_6 in a 60% benzene, 40% benzene-d_6 (by volume) mixture, both at ambient conditions and shock-compressed to 0.91 GPa. Also shown is the 253.652 nm Hg line in second order used as a wavelength reference. The spectral data obtained using RBBCARS shows no evidence for the presence behind the shock of decomposition product species[18] (at concentrations above the 10-20% level) having Raman active transitions within the vibrational frequency region spanned by the gain profile of the dye (i.e. between 800 and 1100 cm^{-1}). In addition, the spectra obtained for the mixtures do not contain any evidence for deuterium exchange reactions between the benzene species during the ~1 ns after passage of the shock. If exchange had occurred, new peaks would be evident between the benzene and benzene-d_6 transitions. Measured vibrational ring-stretching frequency shifts for benzene obtained using RBBCARS and the shifts measured using RSRS as a function of shock pressure are shown in Fig. 8. The data indicates that the two techniques measure equivalent frequency shifts at equivalent shock pressures. Temporal resolution for the
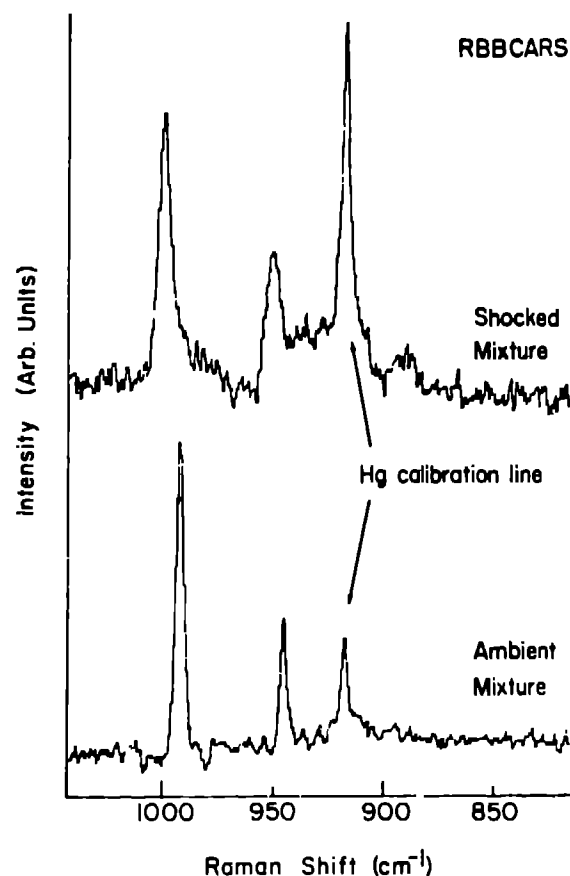

Figure 9. RBBCARS Spectra[24] The Ambient Peak Positions Of The Two Species Are 992 cm^{-1} For Benzene And 945 cm^{-1} For Benzene-d_6.

RBBCARS technique is determined by the laser pulse duration. Since the beam crossing-angles required for phase matching are a few degrees, spatial resolution is somewhat less than the confocal parameter of the focusing lens (Table I). This decrease in spatial resolution from that potentially available with inverse Raman scattering is a distinct disadvantage of CARS and CSRS, and will ultimately be a handicap when trying to measure relaxation phenomena in the region immediately behind the shock-front.

The real advantage of CARS and CSRS experiments is the large scattering intensity and beam-like nature of the signals that enable tremendous discrimination against background fluorescence and emission. CARS also frequency discriminates against fluorescence interference. By proper sample selection, interference from the non-resonant background signals and cross-talk between closely spaced lines can be minimized. Because of the large signal-to-noise ratios expected, detection of

species with concentrations down to part-per-hundred levels should be possible.

Raman-induced Kerr effect spectroscopy (RIKES)[27] has been suggested as a diagnostic technique[21] for performing measurements in shock-compressed systems which may have a large non-resonant background. Similar to inverse-Raman scattering, RIKES requires a single frequency pump beam, a broad-band probe source, no phase match.ng and lower incident power levels than stimulated Raman scattering (Fig. 4). Appropriate polarization of the input pump and probe beams results in a scattered probe beam whose polarization is rotated at conditions of Raman resonance. An analyzer placed in the scattered probe beam thus transmits light only at differences in frequency corresponding to Raman resonances. This arrangement ideally would give a large signal intensity against a small background making it a good choice for the detection of species with small concentrations. In shock applications, however, two difficulties could arise. The strained shock-compressed sample could exhibit birefringence which would rotate the polarization of all of the incident probe frequencies, resulting in a large unwanted background. The second problem arises in geometric arrangement considerations. Since a polarization analyzer is required in the output beam, a straight line transmission arrangement is the most logical choice. A second choice would be similar to Fig. 10 with optical components arranged to null any polarizing effects of the reflecting surface. Temporal and spatial resolutions for such an arrangement should be the laser pulse length and the diffraction limit of the optical components used.

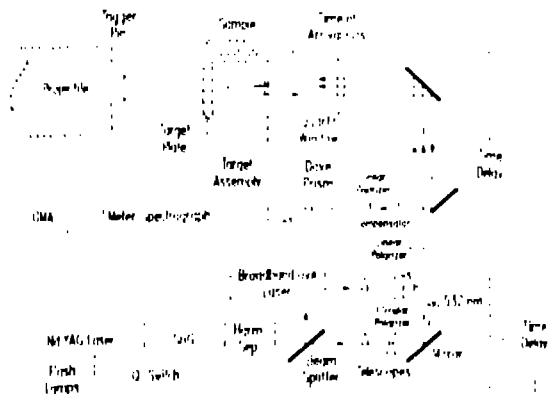Figure 11 shows two RIKES spectra from two different experiments of the 992 cm^{-1} region of benzene shock-compressed to 1.17 GPa. Both traces have spectral features, however they are not consistent and do not exhibit the pressure-induced frequency shift expected for the benzene ring stretching mode based on previous BSRS and RBBCARS experiments. In addition the broadband signal at the dye frequency suggests a shock-induced polarization rotation of the entire probe beam. The conclusion reached from these experiments is that while it may be possible to perform RIKES in shock-compressed materials, the experiment will be considerably more difficult than techniques not requiring polarized laser beams (Table I).

If the output beam of a parametric mixing process is sufficiently strong, it can further mix with one of the incident beams and create a new output beam at yet a different frequency. Higher order Raman spectral excita-

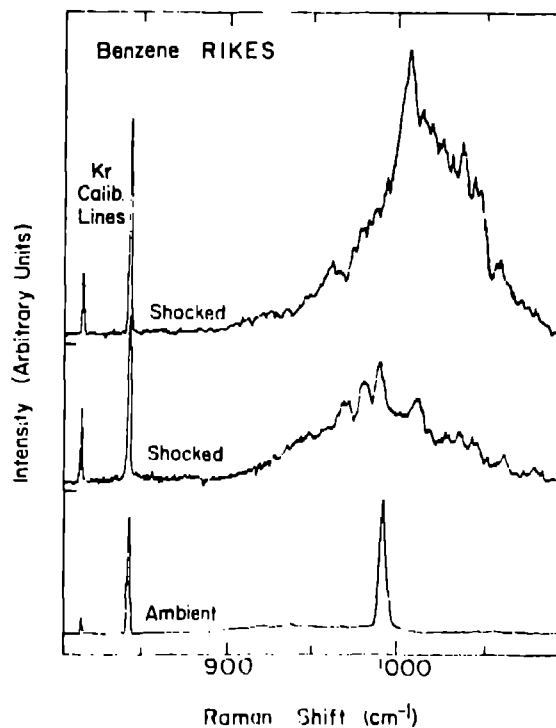Figure 10. Raman Induced Kerr Effect Scattering Experiment.

Figure 11. RIKES Spectra Of Two Shock-Compressed And One Ambient Pressure Benzene Experiments. The Position Of The Ambient Unshifted Vibrational Frequency At 992 cm^{-1} Is Given By The Lower Trace. The Krypton Calibration Lines Are 5570.289 Å And 5562.225 Å.

TABLE I. RAMAN SPECTROSCOPY

Technique	Temporal Resolution (ns)	Spatial Resolution (μ)	Difficulties	Advantages
Incoherent Spontaneous	10	10	Low sensitivity limits temporal and spatial res-	Can identify vibrational spectra and species.
			Difficult in high emission background applications.	Can measure temperature.
			Difficult where fluorescence or photochemistry occurs.	
Resonance	$10^{-4}-10^{4}$	10	May require small species concentrations.	Can identify vibrational spectra and species.
			Could have competing fluorescence effects.	Increased sensitivity compared to spontaneous Raman scattering.
Coherent Stimulated	$10^{-4}-1$	2000	Spatial resolution marginal.	Can identify single vibrational spectra.
			High power levels required.	Good temporal resolution.
			Limited detection capability (single mode and species).	Scattered beam comes back along incident beam.
Inverse	$10^{-4}-10$	10	Appears as a small signal on large background.	Can identify Vibrational spectra and species.
				Does not require phase-matching.
				Good Spatial resolution.
				Good Temporal resolution.
				All Raman active molecules and modes scatter.
				No non-resonant Background.
Anti-Stokes Stokes (CARS,	$10^{-4}-10$	1000	Phase matching required.	Can identify vibrational spectra and species.
				Spatial resolution adequate.
				Good temporal resolution.
				Good detection sensitivity.
				All Raman active molecules and modes scatter.

			Sensitive to birefringence effects.	Can identify Vibrational spectra and species.
Raman Induced Kerr Effect (RIKES)	10^{-4}-10	10		
				L es not require phase matching.
				Good spatial resolution.
				Good temporal resolution.
				All Raman active molecules and modes scatter.
Other			Complicated.	

tion studies (HORSES) (Fig. 4) have been used to generate coherent second Stokes and second anti-Stokes beams. Other multi-color parametric mixing processes using polarized beams have been used to observe Raman transitions. These techniques are generally used to suppress non-resonant background effects. Observation of any of these more complicated processes in shock-compressed systems will probably come after some of the techniques discussed previously are further developed. Optical alignment for any technique requiring polarized beams will surely be difficult.

SUMMARY

Several spontaneous and coherent Raman scattering mechanisms have been discussed as potentially valuable diagnostic techniques for determining the structure and energy transfer mechanisms dominant during the shock compression of condensed-phase molecular systems. The practicality, advantages and disadvantages of each technique have been summarized. Detailed descriptions of backward stimulated Raman scattering and reflected broadband coherent anti-Stokes Raman scattering have been given.

Two fundamental limitations of making experimental measurements in the region through and immediately behind shock fronts are the maximum possible spatial resolution which can be achieved and the increased bandwidth of fast temporal measurements. For visible wavelength optical measurements, the diffraction limit, or spatial resolution, is ~ 1/2 u. For subpicosecond temporal techniques, the bandwidth, or spectral resolution, is tens of wavenumbers.

In the near future, say five years, we believe the evolution of Raman scattering measurements in conjunction with other diagnostic techniques will enable us to perform the following measurements: (1) determination of vibrational energy levels for many shock-compressed materials; (2) identification of material phases when shock-compressed; (3) identification for many materials of chemical species resulting from shock-induced decomposition, polymerization and reaction; (4) de-
termination of reaction-rate phenomenology for shock-compressed materials, (i.e., how do rates and phenomenology change with large compressions and high temperatures); and (5) measurement of some details of shock-front structure possibly providing insight regarding the unique features of the shock process. When the results of these measurements are coupled with presently known information, the possibilities for increasing our phenomenological understanding of the shock-compression process are numerous.

REFERENCES

[1] Kromer, S. B., Optical study of the characteristics of shock-compressed condensed dielectrics, Sov. Phys.-Uspekhi 11, (1968) 229-254.

[2] Davis, W. C., Fine structure in nitromethane/acetone detonations, in Short, J. M. (ed.), Proceedings of the Seventh Symposium on Detonation, Annapolis, Maryland, NSWC MP-82-334 (Naval Surface Weapons Center, White Oak, Maryland, 1981) 953-964.

[3] Schulz, C., Linares, B., Cherville, J. and Poulard, S., Ultra-fast physico-chemical diagnoses of detonation initiation mechanisms. In Proceedings of the Eighth Symposium on Explosives and Pyrotechnics, Los Angeles, California, AD-799 (National Technical Information Service, Springfield, Virginia, 1974) paper 49.

[4] Boisard, F., Tombini, C. and Menil, A., Raman scattering temperature measurement behind a shock wave, in Short, J. M. (ed.), Proceedings of the Seventh Symposium on Detonation, Annapolis, Maryland, NSWC MP-82-334 (Naval Surface Weapons Center, White Oak, Maryland, 1981) 1010-1015.

[5] Delpuech, A., Cherville, J. and Michaud, C., Molecular electronic structure and initiation of secondary explosives. In

Short, J. M. (ed.), Proceedings of the Seventh Symposium on Detonation, Annapolis, Maryland, NSWC MP-82-334 (Naval Surface Weapons Center, White Oak, Maryland, 1981) 65-74.

[6] Tailleur, M. H. and Cherville, J., Etude des condition d'initiation de la pentrite (PETN) par spectrometrie Raman ultra-rapide, Propellants, Expl. and Pyrotech. 7 (1982) 22-27.

[7] Holmes, N., Lawrence Livermore National Laboratory, private communication.

[8] Rousseau, D. L., Friedmand, J. M. and Williams, P. F., The resonance Raman effect, in Weber, A. (ed.), Raman Spectroscopy of Gases and Liquid (Springer-Verlag, Berlin, 1979) 203-252.

[9] Woodruff, W. H. and Farquharson, S., Time-resolved resonance Raman spectroscopy (TR^3) and related vidicon Raman spectrography: vibrational spectra in nanoseconds, in Heiftje, G. M. (ed.), New Applications of Lasers to Chemistry (American Chemical Society Symposium Series 85 American Chemical Society, Washington, DC, 1978) 215-236.

[10] Dallinger, R. F., Farquharson, S., Woodruff, W. H. and Rodgers, M. A. J., Vibrational spectroscopy of the electronically excited state: 4. nanosecond and picosecond time-resolved resonance Raman spectroscopy of carotenoid excited states, J. Am. Chem. Soc. 105 (1978) 7433-7440.

[11] Schmidt, S. C., Moore, D. S., Schiferl, D. and Shaner, J. W., Backward stimulated Raman scattering in Shock-compressed benzene, Phys. Rev. Lett. 50 (1983) 661-664.

[12] Maier, M., Kaiser, W. and Giordmaine, J. A., Backward stimulated Raman scattering, Phys. Rev. 177 (1969) 580-599.

[13] Linde, D. V. D., Maier, M. and Kaiser, W., Quantitative investigations of the stimulated Raman effect using subnanosecond light pulses, Phys. Rev. 178 (1969) 11-17.

[14] Rice, M. H., McQueen, R. G. and Walsh, J. M., Compression of solids by strong shock waves, in Seitz, F. and Turnbull, D. (eds.), Solid State Physics 6 (Academic Press, New York, 1958) 1-63.

[15] Dick, R. D., Shock wave compression of benzene, carbon disulfide, carbon tetrachloride and liquid nitrogen, J. Chem. Phys. 52 (1970) 6021-6032.

[16] Ellenson, W. D. and Nicol, M., Raman spectra of solid benzene under high pressures, J. Chem. Phys. 61 (1974) 1380-1389; this mode is called ν_2 in Herzberg, G. Infrared and Raman Spectra (Van Nostrand Reinhold, New York, 1968) 118.

[17] Keeler, R. N., Bloom, G. H. and Mitchell, A. C., Stimulated Brillouin scattering in shock-compressed fluids, Phys. Rev. Lett. 17 (1966) 852-854.

[18] Dremin, A. N. and Babare, L. V., The shock wave chemistry of organic substances, in Nellis, W. S., Seamen, L. and Graham, R. A. (eds.), Shock Waves in Condensed Matter 1981, Am. Inst. Phys. Proc. 78 (American Institute of Physics, New York, 1982) 27-41.

[19] Jones, W. J. and Stoicheff, B. P., Inverse Raman spectra: induced absorption at optical frequencies, Phys. Rev. Lett. 17 (1964) 657-659.

[20] Yeung, E. S., Spectroscopy by inverse Raman scattering, in Heiftje, G. M. (ed.), New Applications of Lasers to Chemistry, American Chemical Society Symposium Series 85 (American Chemical Society, Washington, DC, 1978) 193-214.

[21] Von Holle, W. G. and McWilliams, R. A., The application of Single-pulse nonlinear Raman techniques to a liquid photoytic reaction, in Crosley, D. R. (ed.), Laser Probes for Combustion Chemistry, American Chemical Society Symposium Series 134 (American Chemical Society Washington, DC, 1980) 319-327.

[22] Maker, P. D. and Terhune, R. W., Study of optical effects due to an induced polarization third order in the electrical field strength, Phys. Rev. 137 (1965) A801-A818.

[23] Tolles, W. M., Nibler, J. W., McDonald, J. R. and Harvey, A. B., A review of the theory and application of coherent anti-stokes Raman spectroscopy (CARS), Appl. Spectrosc. 31 (1977) 253-271.

[24] Moore, D. S., Schmidt, S. C. and Shaner, J. W., Simultaneous multimode pressure-induced frequency shift measurements in shock-compressed organic liquid mixtures by use of reflected broad-band coherent anti-stokes Raman scattering, Phys. Rev. Lett. 50 (1983) 1819-1822.

[25] Roh, W. B., Schreiber, P. W. and Taran, J. P. E., Single-pulse coherent anti-stokes Raman scattering, Appl. Phys. Lett. 29 (1976) 174-176.

[26] Valentini, J. J., Moore, D. S. and Bomse, D. S., Collision-free coherent anti-stokes Raman spectroscopy (CARS) of molecular photofragments, Chem. Phys. Lett. 83 (1981) 217-221.

[27] Heiman, D., Hellworth, R. W., Levenson, M. D. and Martin, G., Raman-induced Kerr effect, Phys. Rev. Lett. 36 (1976) 189-192.